JOURNAL OF MATERIALS SCIENCE 10 (1975) 460–468

A new process for atomization of metal alloys

D. APELIAN*, M. C. FLEMINGS, R. MEHRABIAN
Department of Metallurgy and Materials Science, Massachusetts Institute of Technology, Cambridge, Massachusetts, USA

A laboratory apparatus was constructed to atomize metal alloys by forcing them through sintered ceramic disc filters. The process combines filtration of oxides and/or undesirable second phase particles with atomization. Sintered Al_2O_3 and SiO_2 disc filters with average pore sizes in the range of 36 to 150 μm were used. The effectiveness of various filters in removing "synthetic inclusions" from Al–Ti–B melts was studied. 2 to 10 μm size TiB_2 particles were successfully filtered out. Atomization experiments were done with pure aluminium and 7075 aluminium alloy. Spherical powders, 150 to 2000 μm in size, of 7075 aluminium alloy with secondary dendrite arm spacings between 4 to 8 μm, were cold compacted and extruded into a billet. Room temperature longitudinal properties of the billet in T6 condition were: YS 80 × 10^3 psi†, UTS 94.3 × 10^3 psi, elongation 15% and R.A. 42%.

1. Introduction

An atomization process that combines filtration of metal alloys with powder production will be described. The process entails atomization of an alloy by forcing it through porous ceramic filters. Experiments were carried out on aluminium alloys to determine the governing parameters of the process, and the effectiveness of the filter media in removing inclusions from the melt. An extrusion billet made from these

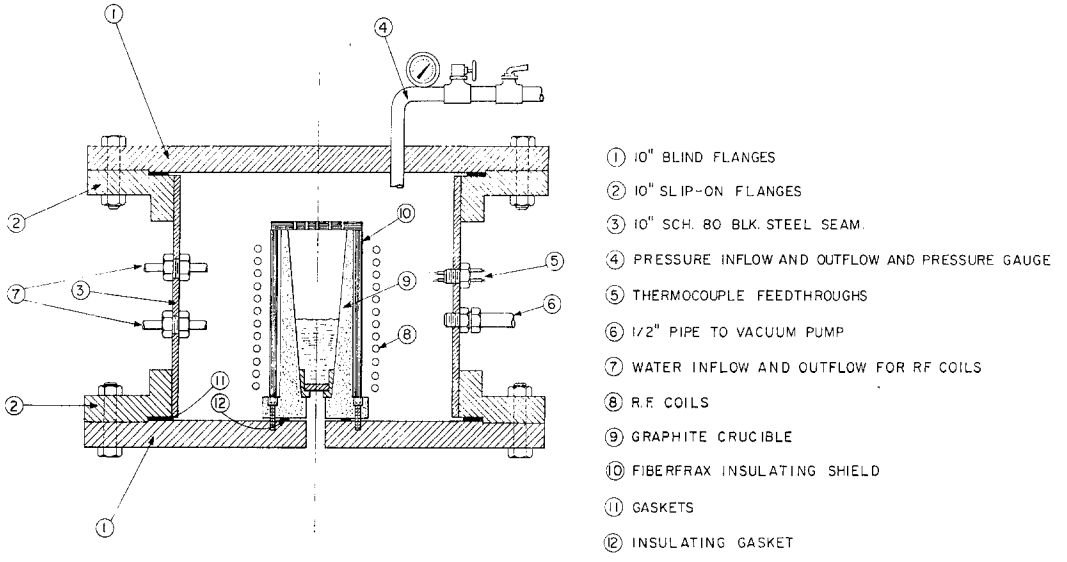

Figure 1 Schematic drawing of apparatus used in this study.

*Present address: Bethlehem Steel Corporation, Homer Research Laboratories, Bethlehem, Pennsylvania.
†10^3 psi = 6.89 N mm^{-2}

TABLE I Procedure and experimental results of filtration of Al–Ti–B alloys

Run no.	C_0–Ti	C_0–B	T_F	C_{NF}–Ti	C_{NF}–B	C_F–Ti	C_F–B	Filter description
35	5.0	1.0	725	6.3	1.3	0.3	0.1	One sintered Al_2O_3, pore size 87 to 100 μm
41b	0.51	0.11	750	0.816	0.162	0.318	0.022	One sintered Al_2O_3, pore size 87 to 100 μm
42b	0.54	0.13	750	1.34	0.34	0.264	0.01	One sintered Al_2O_3, pore size 36 to 40 μm
42d	0.54	0.13	750	1.56	0.30	0.24	0.01	One sintered Al_2O_3, pore size 36 to 40 μm
56	0.54	0.13	750	0.48	0.06	0.37	0.04	One sintered quartz, pore size 90 to 150 μm
57	0.54	0.13	750	0.63	0.140	0.31	0.023	Three sintered quartz, pore size 90 to 150 μm
58	0.54	0.13	685	0.530	0.093	0.24	0.01	One sintered Al_2O_3, pore size 87 to 100 μm

T_F: Filtration temperature (°C).
C_0–Ti, C_0–B: titanium and boron compositions of the initial charge alloy, respectively (wt %).
C_{NF}–Ti, C_{NF}–B: titanium and boron compositions of non-filtered metal above filter, respectively (wt %)
C_F–Ti, C_F–B: titanium and boron compositions of filtered metal, respectively (wt %).

powders was tested for mechanical properties.

In general, for production of high quality powders of many alloys (iron, cobalt, and nickel-base superalloys being examples), surface oxides are undesirable because they cause poor bonding of the particles. Inert gas or hydrogen entrapped as porosity is undesirable because it is compacted at high temperature and hot-pressurized and can subsequently expand in service at high temperature leading to failure of the material. Secondary particles formed in the melt, such as inclusions, are undesirable because they too result in lower mechanical properties of the final part.

Of all the various powder manufacturing processes available the particular process to be described is unique because: (i) filtration of undesired oxides, inclusions, and foreign particles occurs prior to powder drop formation, and (ii) the process can be carried out in high vacuum.

2. Apparatus and procedure

A schematic drawing of the apparatus for the production of metal powders through ceramic filters is shown in Fig. 1. It consists of a pressure vessel within which a crucible is placed containing the metal charge and a filter assembly located below the charge. R.f. induction heating is employed within the chamber. The chamber is 10 in. diameter by 8 in. high. It is placed at a

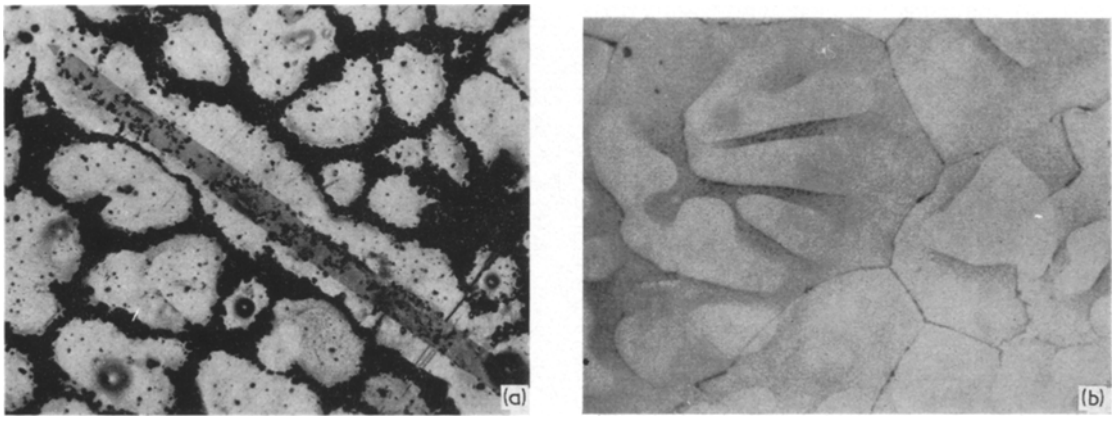

Figure 2 Microstructure of non-filtered and filtered metal from run 35, Table I. (a) Non-filtered metal above the "cake", × 500; (b) filtered metal, × 200.

height of 7 to 8 ft. to allow a long enough free-fall distance for the metal powders to solidify. The liquid metal, which is melted *in situ*, is atomized by pressuring the chamber with an inert gas.

The crucible is mounted on the base of the chamber by six bolts utilizing an asbestos insulating gasket. With this construction, upon pressurization, the crucible is under pressure from all sides except the bottom, and a pressure differential is set within the crucible between the melt and the lower chamber.

The filter media employed (sintered discs of alumina or quartz) is completely contained within a graphite filter assembly, which in turn is mounted in the crucible with a taper fit. Hence, pressurization of the top of the melt forces liquid metal down through the filter (Fig. 1).

Atomization experiments were done with 99.99% aluminium and 7075 aluminium alloy of 7.3% Zn–3.2% Mg–2% Cu–0.25% Cr nominal composition. The effectiveness of the ceramic disc filters in removing particles from a melt, prior to atomization was also studied. TiB_2 "synthetic inclusions", 2 to 10 μm in size, were precipitated from an Al–Ti–B alloy prior to filtration. The non-filtered metal above the disc filter and the filtered metal were chemically analysed and metallographically examined.

Filter materials were Al_2O_3 porous disc filters of 36 to 40 μm and 87 to 100 μm pore sizes and sintered quartz discs of 40 to 90 μm and 90 to 150 μm pore sizes. The filters were $\sim 1\frac{1}{4}$ in. diameter and $\sim 3/16$ in. thickness.

The procedure was to melt about 200 g alloy in a nitrogen atmosphere and superheat it to $\sim$ 900°C. The power was then gradually decreased reducing the melt temperature to a predetermined level, T_F. In the filtration studies the Al–Ti–B phase diagram was utilized, and the temperature T_F was chosen such that coarse $TiAl_3$ and fine TiB_2 particles precipitated in the melt. The melt was held at this temperature for 15 min. Inert gas pressure above the melt was increased to $\sim$30 psi and the emitting liquid streams from below the filter were captured in a copper-chill mould. Table I lists the Al–Ti–B alloys and the filters employed.

In the atomization experiments melt temperature, T_F, was chosen to be above the liquidus temperature of the alloys. The pressure above the melt was gradually increased until metal drops (powders) started to exit from the filter. The pressure differentials employed for successful

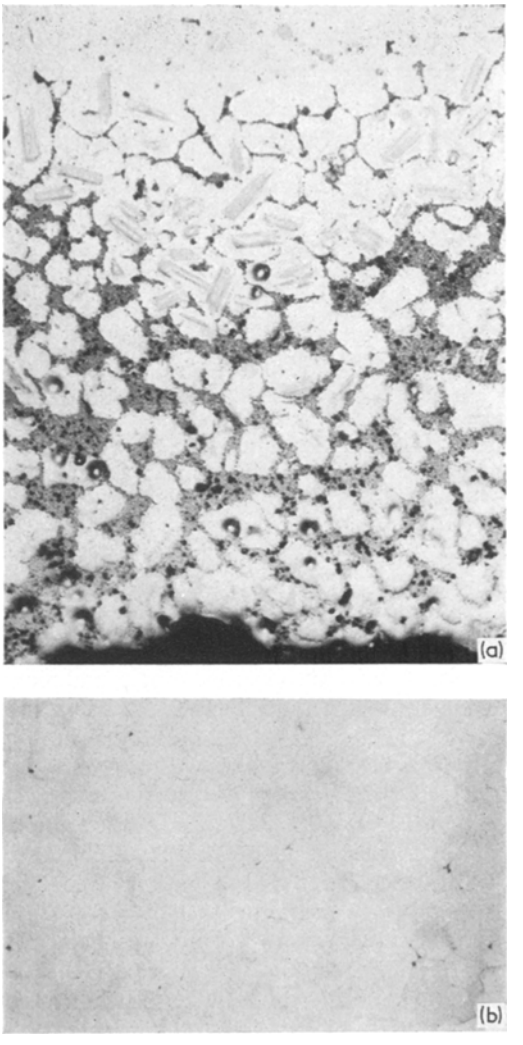

Figure 3 Microstructure of non-filtered and filtered metal from run 58, Table I. (a) "Cake" formed above the filter, platelets are $TiAl_3$ particles, × 75; (b) filtered metal, × 75.

atomization were 2 to 6 psi depending on melt temperature and filter pore size. Size distribution curves of the resulting powders obtained from the various filters were determined by sizing (sieve analysis) and weighing of the powders.

Pound lots of spherical powders of 7075 alloy produced, as described above, were cold compacted under 20 000 psi pressure into a 3 in o.d. by 2 in i.d. 6061-T6 aluminium can. This extrusion billet was heated to a solutionizing temperature of 476°C, held there for 1 h and furnace cooled. Subsequently, it was sealed, soaked at 300°C for 4 h and extruded at the

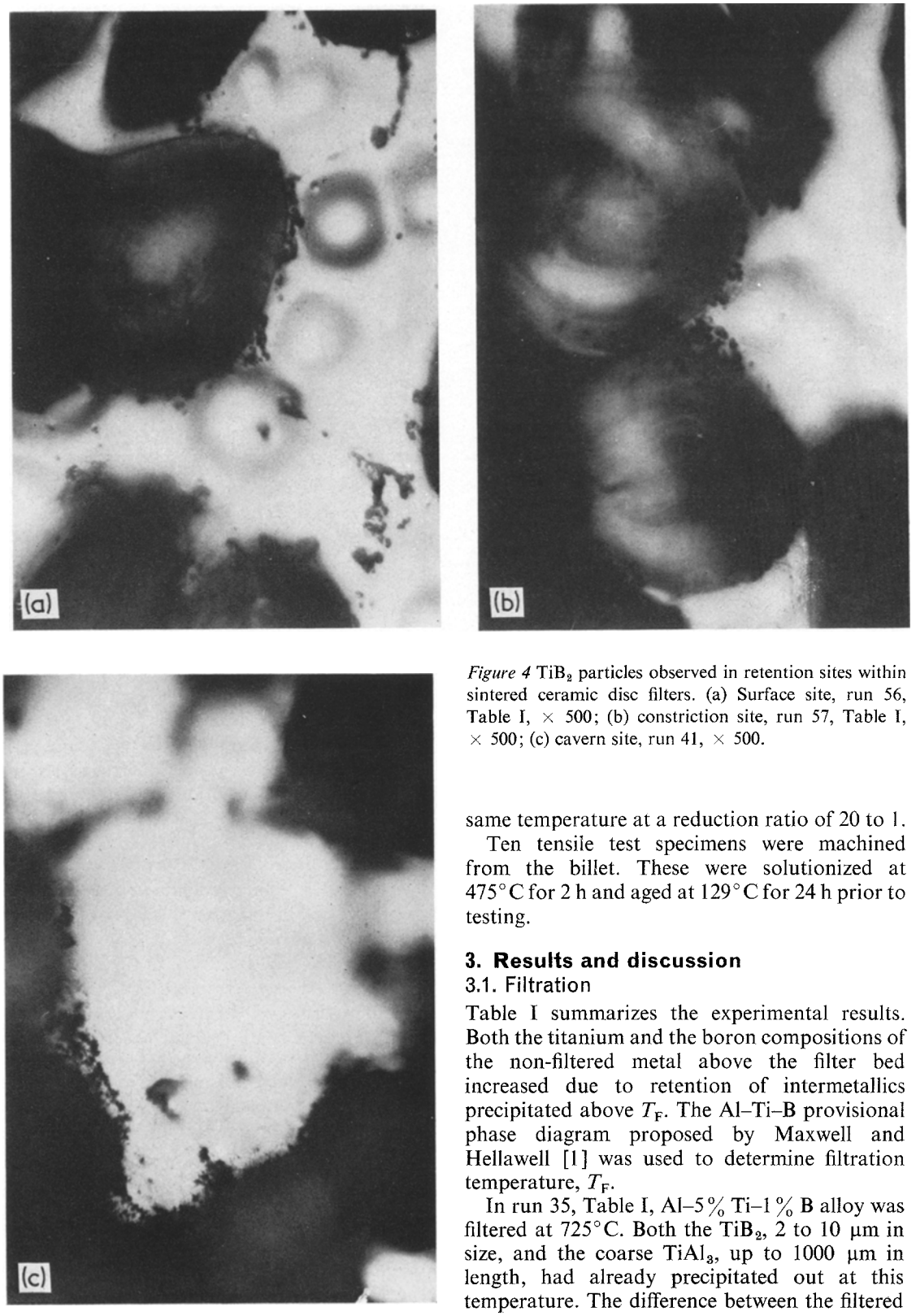

Figure 4 TiB_2 particles observed in retention sites within sintered ceramic disc filters. (a) Surface site, run 56, Table I, × 500; (b) constriction site, run 57, Table I, × 500; (c) cavern site, run 41, × 500.

same temperature at a reduction ratio of 20 to 1.

Ten tensile test specimens were machined from the billet. These were solutionized at 475°C for 2 h and aged at 129°C for 24 h prior to testing.

3. Results and discussion

3.1. Filtration

Table I summarizes the experimental results. Both the titanium and the boron compositions of the non-filtered metal above the filter bed increased due to retention of intermetallics precipitated above T_F. The Al–Ti–B provisional phase diagram proposed by Maxwell and Hellawell [1] was used to determine filtration temperature, T_F.

In run 35, Table I, Al–5% Ti–1% B alloy was filtered at 725°C. Both the TiB_2, 2 to 10 μm in size, and the coarse $TiAl_3$, up to 1000 μm in length, had already precipitated out at this temperature. The difference between the filtered

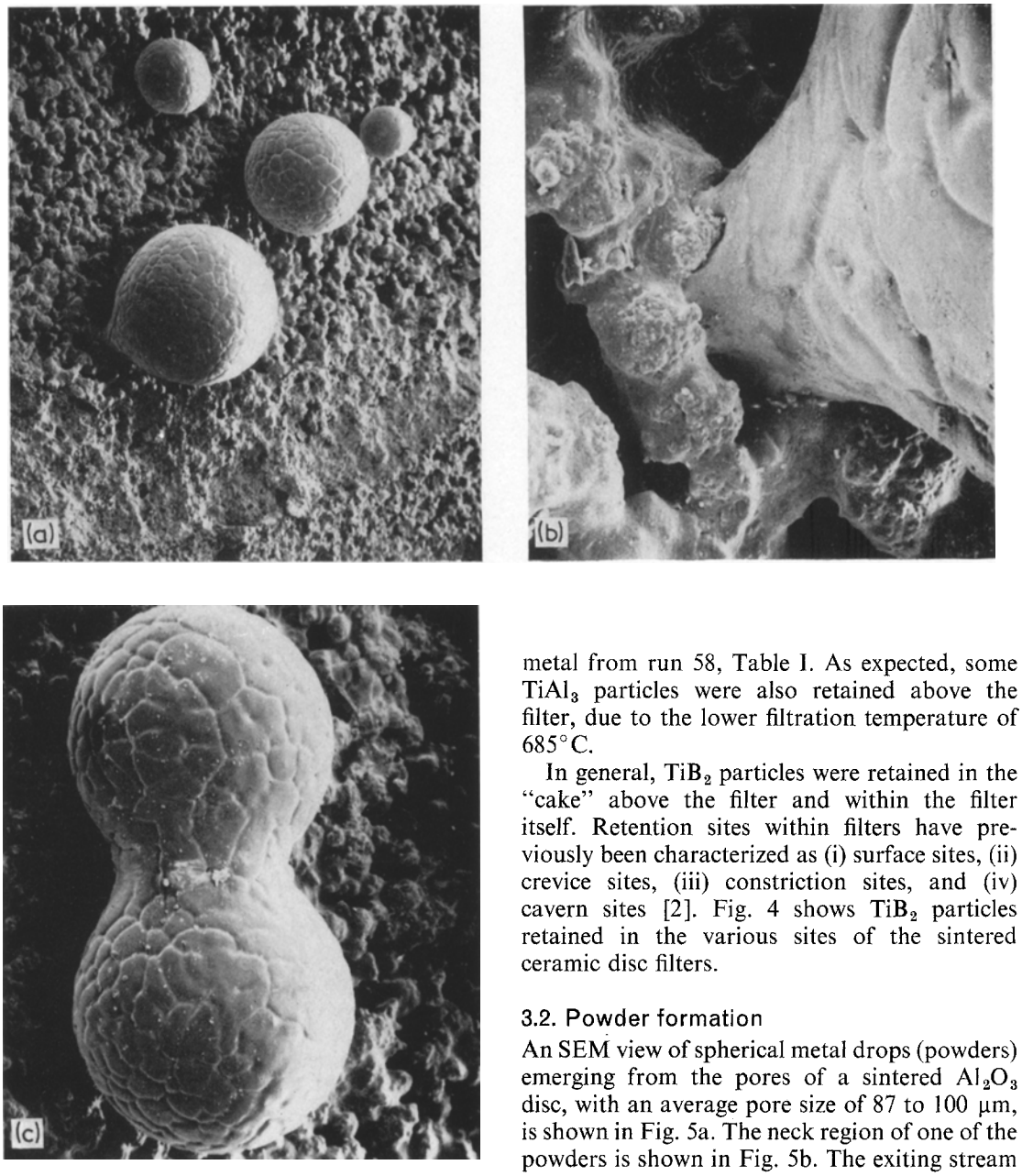

Figure 5 SEM views of pure Al powders emerging from a sintered Al_2O_3 filter. (a) × 23; (b) × 208; (c) × 75.

and non-filtered metals can be seen by comparing the microstructures of Fig. 2a and b.

In the Al–0.5% Ti–0.1% B alloys $TiAl_3$ precipitates out prior to filtration if filtration temperatures is below ~750°C. For example, Fig. 3a and b show microstructures of the "cake" formed above the filter and the filtered metal from run 58, Table I. As expected, some $TiAl_3$ particles were also retained above the filter, due to the lower filtration temperature of 685°C.

In general, TiB_2 particles were retained in the "cake" above the filter and within the filter itself. Retention sites within filters have previously been characterized as (i) surface sites, (ii) crevice sites, (iii) constriction sites, and (iv) cavern sites [2]. Fig. 4 shows TiB_2 particles retained in the various sites of the sintered ceramic disc filters.

3.2. Powder formation

An SEM view of spherical metal drops (powders) emerging from the pores of a sintered Al_2O_3 disc, with an average pore size of 87 to 100 μm, is shown in Fig. 5a. The neck region of one of the powders is shown in Fig. 5b. The exiting stream of liquid metal becomes spherical in shape due to surface tension forces, and subsequently drop detachment occurs. Hauser *et al.* [3] have investigated the steps of formation and detachment of drops from the end of vertical tubes. They show that a waist forms first and rapidly necks down into a stem which then breaks off close to the top of the drop. Harkins and Brown [4] have derived an expression for drop formation using a force balance between gravity and surface tension. These types of analyses, however,

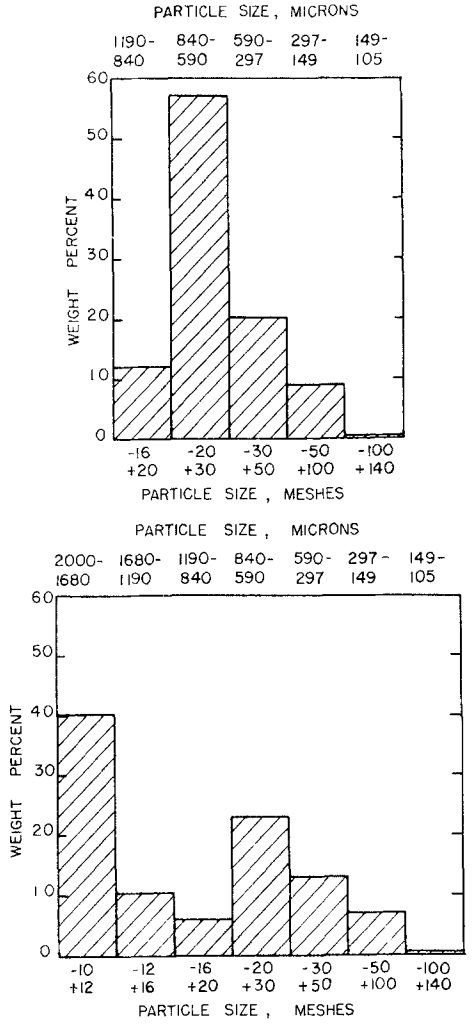

Figure 6 Size distributions of spherical 7075 Al alloy powders made utilizing Al_2O_3 filters with an average pore size of 87 to 100 μm. Melt-temperature (a) $T_F = 700°C$, (b) $T_F = 742°C$.

do not take into account formation of an oxide skin or solidification of the droplet.

Experimental observations showed that successful formation of spherical powder particles depends on detachment of the liquid drops from the filter prior to growth and coalescence of adjacent drops. Conditions that permit liquid drops exiting from adjacent pores to coalesce result in formation of large liquid drops that do not completely solidify in flight and splat in the collector container. The different variables that affect formation and subsequent solidification of the powder particles are: (a) pressure differential across the ceramic filter, (b) superheat in the melt, (c) the wetting angle between the melt and the ceramic filter, and (d) the average pore size of the ceramic filter.

3.2.1. Pressure

A large number of available pores in the bottom of the filter are not utilized during drop (powder) formation (Fig. 5a). Liquid metal preferentially flows through paths of least resistance, causing a channelling phenomenon to occur. Increasing the pressure differential leads to utilization of a greater number of pores. However, increasing the pressure head, above a critical maximum causes consolidation of drops from adjacent pores (i.e. less than one drop diameter apart) (Fig. 5c). In the extreme case, consolidation of many liquid drops results in formation of large drops, or streams, which do not completely solidify in flight and splat against the collection container forming flakes.

3.2.2. Superheat

Direct observations of drop formation through magnifying lenses located below the filter, have shown that formation of consolidated large drops, or streams, can be correlated to superheat in the melt. In general, increasing the superheat in the melt results in formation of larger drops before detachment from the filter occurs. Sieve analysis of spherical powders of 7075 aluminium alloy produced from melts at 700 and 742°C are shown in Fig. 6a and b, respectively.

3.2.3. Wetting

Increased wetting between the ceramic filter and the molten alloy has an adverse effect on successful production of spherical powders. It was found that Al_2O_3 filters were more amenable to atomization than the SiO_2 filters. Liquid aluminium wets SiO_2 much more readily than it does Al_2O_3 [5]. Hence, liquid drops spread out more easily on the SiO_2 filters, leading to formation of consolidated drops.

3.2.4. Filter pore size

The diameters of atomized powders decrease with decreasing average pore size of the filters used. As expected, pressure differentials required are higher for the finer pore filters.

3.3. Structures of atomized powders

Fig. 7a shows an SEM view of 150 to 300 μm size pure aluminium powders made using a 87 to

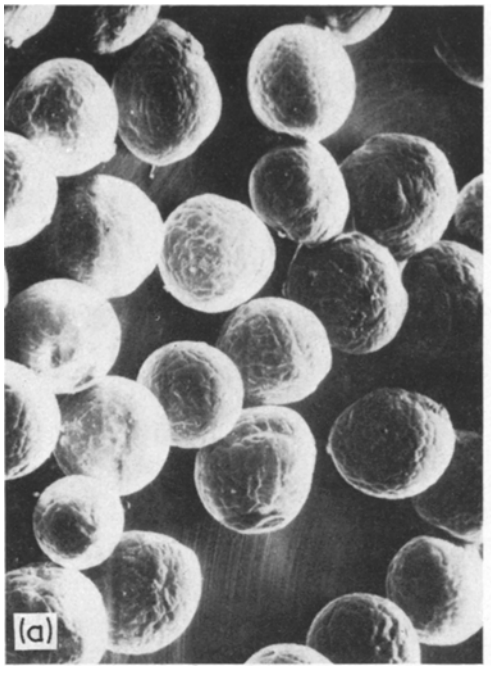

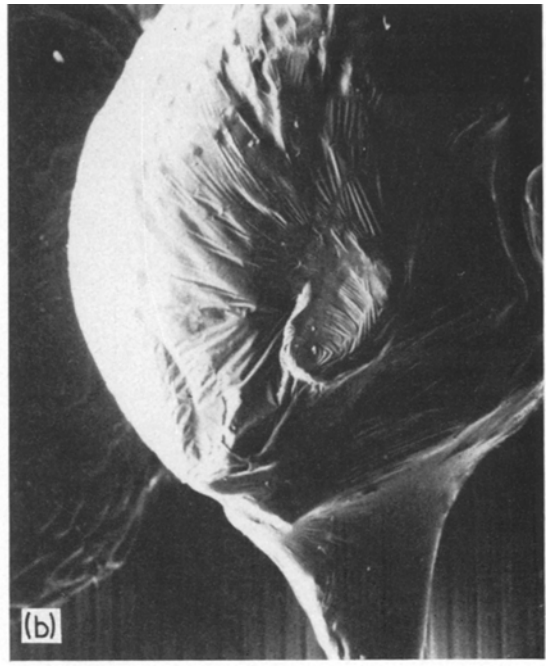

Figure 7 SEM views of atomized pure (99.99%) Al powders made utilizing an Al_2O_3 filter with average pore size of 87 to 100 μm. (a) × 50; (b) and (c) × 590.

100 μm average pore size Al_2O_3 filter. Occasionally powders with stems or tips not completely detached were also observed (Fig. 7b). At a higher magnification, surface irregularities such as ripples, folds, and waves are observed (Fig. 7c). These are caused when the initial oxide layer tries to accommodate deformation experienced by the drop as solidification, shrinkage, and flight instabilities occur.

Fig. 8a and b show an SEM view and a representative microstructure, respectively, of a 7075 aluminium alloy powder. Measured secondary dendrite arm spacings were between 4 to 8 μm, indicating cooling rate of $\sim 10^3$° C sec^{-1} [6].

3.4. Extrusion billets

Spherical powders of the 7075 aluminium alloy ranging in size from 100 to 2000 μm, obtained with the Al_2O_3 filters were cold-compacted and hot-extruded into a billet. The billet was heat-treated to a T6 condition as previously described. The transverse and longitudinal microstructures of the extruded billet are shown in Fig. 9.

Room temperature average tensile properties, from multiple tests in the longitudinal direction, were: YS = 80 × 10^3 psi, UTS = 94 × 10^3 psi, elongation = 15%, R.A. = 42%.

4. Conclusions

(1) A new process for production of metal alloy powders was developed. The process combines

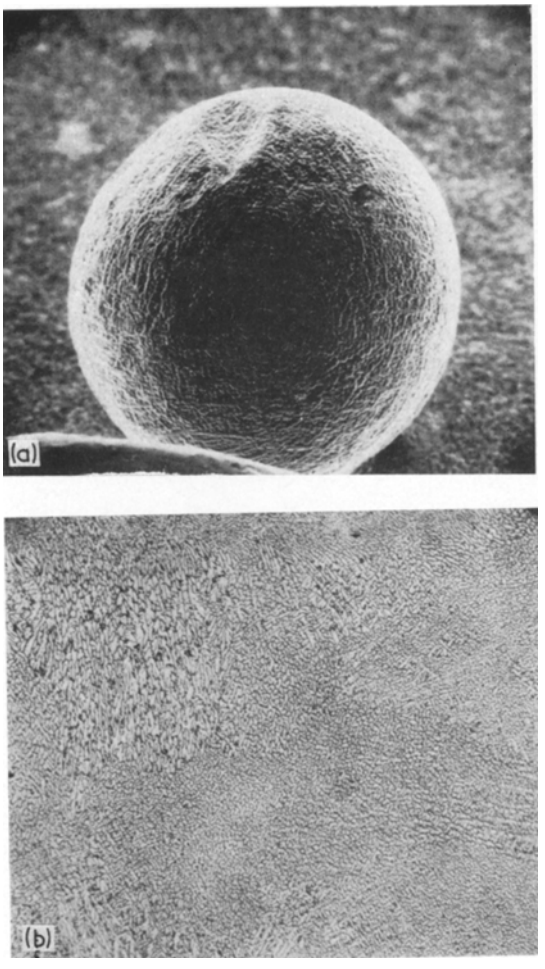

Figure 8 Atomized powder of 7075 Al alloy made utilizing an Al_2O_3 filter with average pore size of 87 to 100 μm, – applied pressure and melt temperature 5 psi and 745° C, respectively. (a) SEM view, × 110, (b) photomicrograph of a polished and etched cross-section, × 100.

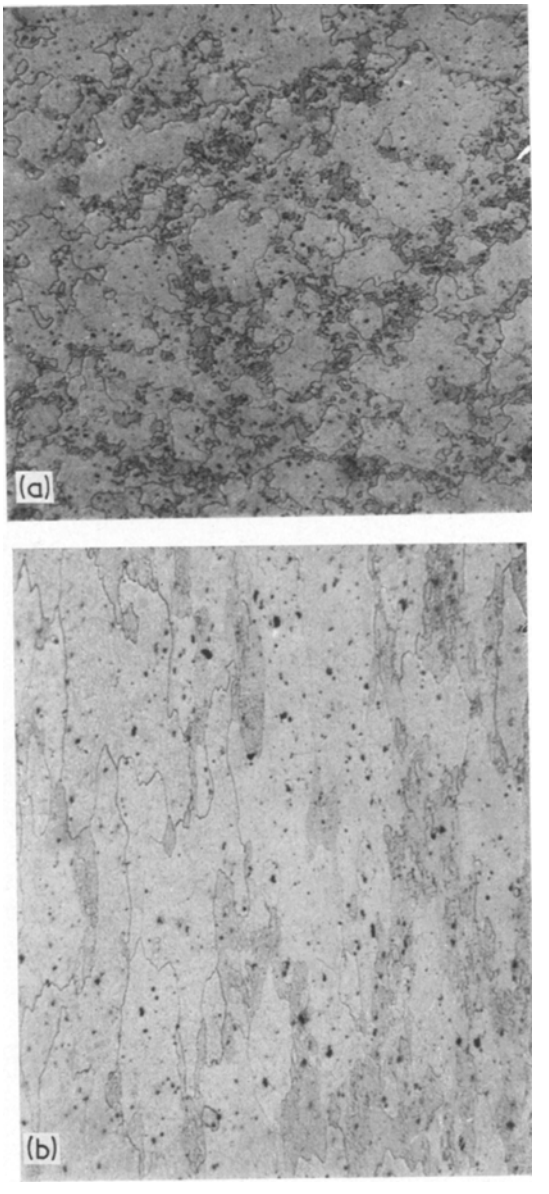

Figure 9 Microstructure of 7075-T6 extrusion made from atomized spherical powders, × 100. (a) and (b) are transverse and longitudinal cross-sections, respectively.

filtration of oxides and undesirable second phases with atomization. Sintered Al_2O_3 and SiO_2 disc filters with pore sizes in the range of 30 to 150 μm were used.

(2) TiB_2 "synthetic inclusions" of 2 to 10 um size range were successfully filtered from Al–Ti–B alloys. The particles either accumulated above the filter and formed a "cake", or were entrapped at retention sites within the filters.

(3) Pure aluminium and 7075 aluminium alloy were atomized by forcing them through the sintered ceramic disc filters. The Al_2O_3 filters were found to be more amenable to successful droplet formation.

(4) For a given sintered disc filter successful formation of metal powders below the filter is a critical function of the pressure differential across the filter. Pressure differentials used in this study were in the range of 2 to 6 psi.

(5) Size range of powders is influenced by the amount of superheat in the melt. Increasing superheat results in formation of larger powders.

(6) The longitudinal room temperature tensile

properties of a 7075-T6 extrusion made from the atomized powders were: YS = 80 × 10^3 UTS ≃ 94 × 10^3 psi, elongation = 15%, R.A. = 42%.

Acknowledgement

The authors acknowledge financial support by the Advanced Research Projects Agency of this research programme.

References

1. I. MAXWELL and A. HELLAWELL, *Met. Trans.* **3** (1972) 148.
2. J. P. HERZIG, D. M. LEIPERC and P. LEGOFF, "Flow Through Porous Media" (American Chemical Society Publication, Washington, D.C. 1970).
3. E. A. HAUSER, H. E. EDGERTON, B. M. HOLT and J. T. COX, *J. Phys. Chem.* **40** (1936) 973.
4. W. D. HARKINS and F. E. BROWN, *J. Amer. Chem. Soc.* **41** (1919) 499.
5. W. D. KINGERY, *J. Amer. Ceram. Soc.* **37** (1954) 44.
6. H. MATYJA, B. C. GIESSEN and N. J. GRANT, *J. Inst. Metals* **96** (1968) 30.

Received 29 August and accepted 9 September 1974.